HHS Public Access

Author manuscript

Nat Immunol. Author manuscript; available in PMC 2012 March 11.

Published in final edited form as:

Nat Immunol. ; 12(8): 733–741. doi:10.1038/ni.2069.

Essential role for the prolyl isomerase Pin1 in Toll-like receptor signaling and type I interferon-mediated immunity

Adrian Tun-Kyi[1,*], **Greg Finn**[1,*], **Alex Greenwood**[2], **Michael Nowak**[1], **Tae Ho Lee**[1], **John M. Asara**[1], **George C. Tsokos**[1], **Kate Fitzgerald**[3], **Elliot Israel**[4], **Xiaoxia Li**[5], **Mark Exley**[1], **Linda K. Nicholson**[2], and **Kun Ping Lu**[1,†]

[1]Department of Medicine Beth Israel Deaconess Medical Center Harvard Medical School Boston, MA 02215, USA

[2]Department of Molecular Biology and Genetics Cornell University Ithaca, NY 14853, USA

[3]Division of Infectious Diseases and Immunology University of Massachusetts Medical School Worcester, Massachusetts 01605, USA

[4] Department of Medicine Brigham and Women's Hospital Boston, MA 02115, USA

[5]Departments of Immunology Cleveland Clinic Foundation Cleveland, Ohio 44195, USA

Abstract

Toll-like receptors (TLRs) shape innate and adaptive immunity to microorganisms. The enzyme IRAK1 transduces signals from TLRs, but its activation and regulation mechanisms remain unknown. We show that TLR7 and TLR9 activated the isomerase Pin1, which then bound to IRAK1, resulting in IRAK1 activation and facilitating its release from the receptor complex to activate the transcription factor IRF7 and induce type I interferons. Consequently, Pin1-null cells and mice failed to mount TLR-mediated, interferon-dependent innate and adaptive immune responses. Given the critical role of aberrant IRAK1 activation and type I interferons in various immune diseases, controlling IRAK1 activation via Pin1 inhibition may represent a useful therapeutic approach.

Toll like-receptors (TLRs) recognize distinct pathogen-associated molecular patterns and elicit signaling cascades, leading to upregulation of type I interferons (IFNs) and proinflammatory cytokines to orchestrate innate and adaptive immunity against infection[1-3]. In particular, the intracellular TLRs are primarily involved in the recognition of viral (TLR3, TLR7) as well as viral and bacterial (TLR9) antigens and are especially adept at triggering type I IFN immune responses[4-7]. While TLR3 ligation induces IRF3 activation and subsequent interferon-β (IFN-β) secretion independent of the adaptor MyD88 but dependent on the adaptor TRIF, the TLR9 subfamily members TLR7 and TLR9 exclusively utilize MyD88, leading to robust type I IFN production mainly from plasmacytoid dendritic cells

---

†All correspondence should be addressed to Kun Ping Lu, Center for Life Science 0408, Beth Israel Deaconess Medical Center, Harvard Medical School, 3 Blackfan Circle, Boston, MA 02115; Tel, 617-735-2016; Fax, 617-735-2050; klu@bidmc.harvard.edu..

*These authors contributed equally to this work

(pDCs)[2, 8]. Type I IFNs are essential for antiviral immune responses as they induce various IFN-inducible genes, promote natural killer cell cytotoxicity, dendritic cell (DC) maturation, and differentiation of virus-specific cytotoxic T lymphocytes, thereby linking innate and adaptive immunity[1-3, 9]. However, TLR activation is a 'double-edged sword', as inappropriate activation can participate in pathologic inflammation and diseases[10, 11].

An essential molecule transducing signals from the upstream receptor complex for most TLRs to downstream transcription factors is the enzyme IRAK1 (IL-1 receptor associated kinase-1)[12-14]. Upon TLR ligation, IRAK1 is recruited to the TLR complex containing MyD88, IRAK4 and the adaptor TRAF6, where IRAK4 phosphorylates IRAK1 promoting IRAK1 autophosphorylation, leading to a characteristic ~20 kDa mobility shift in SDS-containing gels, a hallmark of IRAK activation. Activated IRAK1 dissociates from the receptor complex to activate IRF7 for induction of type I IFNs[12-19]. IRAK1-null mice show a blunted inflammatory response to TLR2 and TLR4 ligation[20], but perhaps their most significant phenotype is the complete loss of IFN-α secretion following TLR7 or TLR9 ligation[14]. Although IRAK1 autophosphorylation is implicated as a key event in TLR signaling[12, 13, 17], little is known about how such phosphorylation leads to IRAK1 activation and whether there is further regulation following phosphorylation.

Protein phosphorylation on serine or threonine residues preceding proline (Ser/Thr-Pro) is a central signaling mechanism in many cellular processes under both physiological and pathological conditions[21]. pSer/Thr-Pro motifs exist in two distinct *cis* and *trans* conformations, whose inter-conversion rate is markedly slowed down upon phosphorylation, but specifically accelerated by the unique prolyl isomerase Pin1[22]. Pin1 has two structurally and functionally distinct domains, a pSer/Thr-Pro-binding WW domain and pSer/Thr-Pro-isomerizing catalytic domain. Pin1 controls the function of many key regulators in various cellular processes and its deregulation contributes to the pathogenesis of a growing number of diseases[21].

Pin1 acts on IRF3 to affect IFN-β production upon TLR3 or activation of the helicase RIG-I [23]. However, unlike IRF3- or TLR3-deficient mice, IRF7 or IRAK1-deficient mice completely fail to mount a type I IFN antiviral responses due to particular loss of type I IFN secretion from pDCs[19, 24]. These findings compelled us to examine the role of Pin1 in other TLR signal pathways. We show that Pin1 is a regulator of IRAK1 activation in TLR signaling and type I IFN-mediated innate and adaptive immunity. Pin1 inhibitors, which are under active development[21, 25], may be useful in allowing selective inhibition of the type I IFN response while leaving proinflammatory cytokine production unaffected.

Results

Pin1 is essential for TLR-induced type I IFN secretion

To examine the role of Pin1 in TLR signaling, we first compared cytokine production in response to various TLR ligands using DC subsets derived from Pin1 wild-type (WT) and Pin1 knockout (KO) mice. When stimulated with LPS (TLR4 ligand), Pam3 CSK4 (TLR2), R-848 (TLR7) or CpG DNA (TLR9), *Pin1* KO myeloid DCs (mDCs) produced moderately less proinflammatory cytokines than *Pin1* WT controls (**Fig. 1a-c**). Consistently, reduced

proinflammatory cytokine secretion was also detected in *Pin1* KO macrophages following stimulation of *Pin1* WT and KO cells with each of the TLR ligands (**Supplementary Fig. 1a, b**). Stimulation of splenic plasmacytoid DCs (pDC) or Flt3 ligand–induced bone marrow pDCs with purified TLR7 or TLR9 ligand or with the influenza A virus (H1N1, a TLR7 stimulator) or mouse cytomegalovirus (MCMV, a TLR9 stimulator) showed robust IFN-α secretion in Pin1 WT cells **(Fig. 1d-g)**, as shown[6, 26]. However, *Pin1* KO cells almost completely failed to produce type I IFNs as measured by ELISA and quantitative RT-PCR analyses (**Fig. 1d-h**) . These effects of *Pin1* deficiency on IFN-α production were highly specific because *Pin1* KO neither affected the population of immune cells nor their TLR expression **(Supplementary Fig. 2)**. Moreover, Pin1 enzymatic activity, although not protein amounts, was significantly elevated in R-848- or CpG-stimulated human peripheral blood mononuclear cells **(Fig. 1i)**, which is consistent with the findings that Pin1 is kept inactivated until cellular cues are engaged[21, 27]. Thus, Pin1 plays a moderate role in proinflammatory cytokine production in mDCs in response to various TLR ligands, but is essential and specific for the type I IFN response in pDCs following TLR7 and TLR9 ligation.

Pin1 interacts with IRAK1 upon TLR stimulation

To elucidate the molecular mechanism underlying the impact of Pin1 on type I IFN secretion, we used a proteomic approach to identify Pin1 substrates using a GST-Pin1 affinity purification procedure under high-salt and -detergent conditions[22, 28], a procedure that has been used to identify almost all known Pin1 substrates[21]. We used R-848-stimulated human THP1 cells, a monocytic cell line that has a functional IFN response to TLR7 and TLR9 ligands and can be cultured in sufficient volumes. Following SDS-PAGE and mass spectrometry, one prominent and reproducible Pin1-binding protein at 100 kDa was identified to be IRAK1 **(Fig. 2a, Supplementary Fig. 3a)**. The *Pin1* KO phenotypes were strikingly similar to those observed in *Irak1* KO cells and mice[14, 20, 29]. Furthermore, similar to *Irak1* KO[14], no obvious effect of *Pin1* deficiency on IL-6 and IL-12p40 protein could be detected following pDCs stimulated with R-848 or CpG **(Supplementary Fig. 1c, d)**. No difference was observed for IFN-β secretion from *Pin1* WT and KO mDCs stimulated with CpG **(Supplementary Fig. 1e)**, which is consistent with the previous results that CpG stimulation of mDCs induces IFN-β production in a MyD88- and IKKα-dependent but IRAK1-independent manner[29]. These results prompted us to examine the role of Pin1 in regulating IRAK1 function in TLR signaling. We confirmed the TLR7 and TLR9-dependent interaction between IRAK1 and Pin1 in THP1 monocytes and RAW264.7 macrophages by GST-Pin1 binding assay **(Fig. 2b)** or co-immunoprecipitation (Co-IP) **(Fig. 2c)**. Pin1 predominantly bound to the activated form of IRAK1, which displayed a characteristic mobility shift on SDS gels after TLR ligation **(Fig. 2b, c, solid arrows)**, suggesting that Pin1 might bind specifically to phosphorylated IRAK1. Indeed, this binding was mediated by the Pin1 WW domain **(Supplementary Fig. 3b, c)**, a known pSer/Thr-Pro-binding module[28], but was abolished either by IRAK1 dephosphorylation prior to Pin1 binding assay **(Fig. 2d, Supplementary Fig. 3d)** or mutating a key functional residue in the WW domain[28]**(Supplementary Fig. 3b, e)**. In addition, Pin1 did not bind to the related kinases IRAK2 and IRAK4 following TLR7 and TLR9 stimulation **(Supplementary Fig. 3f)**. Thus,

following TLR7 or TLR9 ligation, Pin1 is activated and IRAK1 is phosphorylated, which allows Pin1 to interact specifically with IRAK1.

The binding of Pin1 to IRAK1 was somewhat surprising because Pin1 interacts only with specific pSer/Thr-Pro motifs[21, 28] and there is little known about Pro-directed phosphorylation of IRAK1 in TLR signaling[17]. Consequently, we decided to define the Pin1 binding region and site(s) in IRAK1. Structurally, IRAK1 consists of an N-terminal death domain, a ProST-rich undetermined domain (UD) and a central kinase domain, with a C-terminal tail[17]**(Supplementary Fig. 4a)**. To avoid interference of endogenous IRAK1, we expressed FLAG-IRAK1 or its mutants in IRAK1 null (I1A) 293 cells[30], followed by a Pin1 binding assay. Overexpression of IRAK1, but not its K239S kinase-dead (KD) mutant, resulted in its auto-activation independently of TLR stimulation, as indicated by the characteristic mobility shift **(Fig. 2e-gSupplementary Fig. 4b)**, as shown previously[12, 13, 17]. IRAK1, but not its KD mutant, interacted with Pin1 **(Fig. 2e-h, Supplementary Fig. 4b)**. Furthermore, deletion of the UD abolished Pin1 binding **(Supplementary Fig. 4b)**. These data suggest that Pin1 binds to kinase-active IRAK1, possibly through autophosphorylation sites in the UD.

To demonstrate that Pin1 binds to autophosphorylated IRAK1, we co-expressed FLAG tagged KD-IRAK1 with or without WT-IRAK1 in IRAK1-deficient cells, followed by analyzing Pin1 binding specifically to KD-IRAK1. As shown previously[12], KD-IRAK1 did not show the characteristic mobility shift and failed to interact with Pin1 when it was expressed alone **(Fig. 2e left)**. However, when co-expressed with WT-IRAK1, KD-IRAK1 showed the mobility shift and also bound to Pin1 **(Fig. 2e right)**, suggesting that Pin1 binds to autophosphorylated IRAK1. To confirm that Pin1 directly binds to IRAK1, we next performed Far-Western blotting analysis using WT and KD IRAK1 and GST-Pin1 WW domain. Indeed, Pin1 bound only to the slower mobility-shifted and presumably activated form of WT IRAK1, but there was no binding between Pin1 and KD IRAK1 **(Fig. 2f)**. Finally, to confirm the binding of Pin1 to the active form of IRAK1, we performed a Pin1 binding assay using mouse embryonic fibroblasts (MEFs) stably transfected with WT and KD IRAK1 in the presence or absence of TLR7 activation. Pin1 bound to the active form of WT IRAK1, but not KD IRAK1 confirming that Pin1 predominately binds to activated IRAK1 **(Fig. 2g)**. Taken together, these results indicate that upon TLR ligation, IRAK1 is activated by receptor recruitment and autophosphorylates on the pSer-Pro motifs, which in turn recruits Pin1 to act on IRAK1.

To identify the IRAK1 phosphorylation site(s) responsible for Pin1 binding, we mutated each of the six possible Pin1 binding pSer/Thr-Pro motifs in the UD of IRAK1 to Ala, and assessed their binding to Pin1 from retrovirally transfected cells. Although the mutation of S110, S163 or S196 had little effect on Pin1 binding, the mutation of S131, S144 or S173 alone to Ala considerably reduced IRAK1 activation and Pin1 binding, which was further reduced when all three sites were mutated together **(Fig. 2h)**, indicating that phosphorylation of these sites participate in regulating IRAK1 activation and Pin1 binding. To confirm the phosphorylation status of these three sites, we used a two-step purification procedure to isolate IRAK1 using sequential FLAG immunoprecipitation and GST-Pin1 pulldown, followed by liquid chromatography–tandem mass spectrometry (LC-MS/MS) analysis. Both

S131 and S144 were indeed phosphorylated **(Supplementary Fig 5a, b)**. However, both trypsin and chymotrypsin digestions repeatedly failed to produce any peptides covering the region surrounding S173 **(Supplementary Fig 5c)**, possibly due to the numerous proline and hydrophobic residues in this region. This prompted us to generate phospho-specific antibodies against phosphorylated S173 of IRAK1. The resulting anti-pS173 antibodies specifically recognized activated WT IRAK1, but not its S173A point mutant, even when it was highly overexpressed and activated using transient transfection, confirming that S173 in the UD of IRAK1 is indeed phosphorylated **(Supplementary Fig. 6a)**. Moreover, S173 phosphorylation of IRAK1 was significantly induced in R-848- or CpG-stimulated human peripheral blood mononuclear and THP1 monocytes, as determined by flow cytometric **(Fig. 2i)** and immunoblotting **(Supplementary Fig. 6b)** analyses using pS173-specific IRAK1 antibodies. Taken together, these results indicate that upon TLR activation, S131-, 144-, and 173-Pro motifs in the UD of IRAK1 are not only phosphorylated in cells, but also are largely responsible for Pin1 binding.

Pin1 binds to multiple pSer-Pro motifs in IRAK1

The Pin1 WW domain and isomerase (PPIase) domains have been shown to bind and isomerize specific pSer/Thr-Pro motifs in its substrates, respectively[22, 28, 31]. To measure the Pin1 interaction with each of the implicated pSer-Pro motifs in IRAK1, we employed two-dimensional (2D) NMR spectroscopy to monitor the changes in the ^{15}N-WW domain induced by titration with phosphopeptide ligands. In a 2D ^{15}N-^{1}H HSQC spectrum of a protein **(Fig. 3a)**, each backbone NH group is represented by a peak, whose position reflects the chemical environment of that NH bond. Ligand binding to the protein is detected by changes in peak positions (fast exchange) or by the appearance of new peaks (slow exchange) as ligand is added. WW binding at each distinct IRAK1 site was measured using phosphopeptides containing residues 126-136 (pSer131-P132), 140-150 (pSer144-P145), and 157-180 (pSer173-P174) of IRAK1. The WW domain bound to each phosphopeptide and exhibited fast exchange kinetics, as demonstrated by changes in peak position, in each of the three titration experiments **(Fig. 3a)**. Quantitative analysis of the change in chemical shift as a function of peptide concentration **(Fig. 3b)** yielded dissociation constants (K_D) of 220 ± 15 μM, 120 ± 12 μM, and 260 ± 75 μM for the 126-136 (pSer131-P132), 140-150 (pSer144-P145), and 157-180 (pSer173-P174) phosphopeptides, respectively. The IRAK1-Pin1 interaction in the cell occurs as part of a multi-protein membrane-associated complex[12-14], suggesting the potential for significant binding enhancement due to avidity.

In order to determine whether Pin1 catalysis occurs at each of these sites, homonuclear 2D ROESY NMR was used as previously reported[32]. In the presence of a catalytic amount of Pin1, exchange crosspeaks between the *cis* and *trans* isomers of the pSer-Pro peptide bond were clearly observed for each peptide **(Fig. 3c, top panels)**. Conversely, in the absence of Pin1, exchange crosspeaks were missing **(Fig. 3c, bottom panels)**. These results demonstrate that Pin1 accelerates the *cis-trans* isomerization at each pSer-Pro motif, thereby confirming these sites as Pin1 substrates.

Pin1 is essential for IRAK1 activation upon TLR ligation

Given that Pin1 binds to and isomerizes multiple pSer-Pro motifs in IRAK1 upon TLR activation, a key question is whether Pin1 regulates IRAK1 function in TLR signaling. Therefore, we examined the effects of *Pin1* KO on IRAK1 activation in response to activation of various TLRs using *Pin1* WT and KO MEFs and pDCs. Although TLR7 and TLR9 ligation activated IRAK1 in a time-dependent fashion in both Pin1 WT cells **(Fig. 4a)**, as indicated by the mobility shift and increased kinase activity (Fig 4b), as previously described[12, 13, 17], there was no evidence for IRAK1 activation in either assay in *Pin1* KO MEFs or pDCs **(Fig. 4a, b)** or in *Pin1*-silenced THP1 cells using RNAi **(Fig. 4c)**. Moreover, *Pin1* KO also completely abolished IRAK1 activation in response to ligation of other TLRs including TLR2 and TLR4 **(Supplementary Fig. 7a, b)**. These effects were highly specific because *Pin1* KO did not affect activation of the IRAK1 upstream kinase IRAK4 **(Fig. 4b)**, or mitogen-activated protein kinases (MAPK) including ERKs, JNKs and p38 MAPKs upon TLR activation **(Supplementary Fig. 8)**. Similar observations were made following LPS stimulation of macrophages **(Supplementary Fig. 9a)**. We also assessed the effects of Pin1 deficiency on IκB degradation following pDC stimulation with R-848 and CpG or treatment of macrophages with LPS and did not see any obvious difference between *Pin1* WT and KO cells **(Supplementary Fig. 9b, c)**. To further confirm this effect of Pin1 on IRAK1 activation, we developed an assay to measure the kinase activity of IRAK1 in cells utilizing the fact that IRAK1 can phosphorylate the N-terminal 220 amino acid IRAK1 fragment containing the UD in *trans*, as shown by the characteristic mobility shift after co-expression with WT IRAK1 **(Fig. 4d)**, as demonstrated previously[12, 13, 17]. As expected, exogenously-expressed IRAK1 in *Pin1* WT MEFs efficiently phosphorylated the IRAK1 N-terminal fragment, inducing the characteristic mobility shift **(Fig 4d)**. However, like KD *Irak1*, WT *Irak1* in *Pin1* KO MEFs completely failed to induce any mobility shift of the N-terminal IRAK1 **(Fig. 4d)**. These results together indicate that Pin1 is required for IRAK1 activation.

To further demonstrate the importance of Pin1 for the time-dependent activation of IRAK1 following TLR ligation, we overexpressed WT *Irak1* and KD *Irak1* in *Pin1* WT and KO MEFs using a retroviral expression system. Under overexpression conditions, WT-IRAK1 was partially activated, which was further activated upon TLR7 ligation in Pin1 WT cells, as shown by the characteristic mobility shift **(Fig. 4e)**, consistent with the findings that IRAK1 activation is sensitive to the amount of IRAK protein[13, 17]. However, no IRAK1 activation was observed in *Pin1* KO cells, even after stimulation **(Fig. 4e)**, further confirming the role of Pin1 in IRAK1 activation. Importantly, KD IRAK1 did not show any evidence of activation following TLR ligation both in *Pin1* WT and KO cells **(Fig. 4e)**. These results indicated that IRAK1 failed to be activated in *Pin1* KO cells. To confirm that defective IRAK1 activation in *Pin*1 KO cells is specifically due to loss of Pin1 and to examine the importance of Pin1 binding and isomerase activities for IRAK1 activation, we performed rescue experiments by re-expressing WT Pin1 or its point mutants, W34A mutant (in the WW domain) or K63A mutant (in the catalytic domain), which fail to bind to or isomerase Pin1 substrates, respectively[22, 28]. Re-expression of Pin1, but neither of its WW domain (W34A) nor catalytic domain (K63A) point mutant, completely restored IRAK1 activation in *Pin1* KO cells expressing IRAK1 **(Fig. 4f)**, reminiscent of IRAK1 activation found in

Pin1 WT cells **(Fig. 4e)**. Taken together, these results demonstrate an essential role for Pin1 in IRAK1 activation during TLR signaling.

Pin1 is essential for IRAK1-mediated IRF7 activation

Given that Pin1 was required for activation of IRAK1 we wondered whether Pin1 regulates IRAK1 mediated downstream signaling. Following TLR activation, IRAK1 is recruited to the receptor complex via MyD88 and IRAK4, where it is activated and released from the receptor complex. This allows transcription factors such as IRF7, the master regulator of IFN-α, to translocate into the nucleus and activate IFN-α transcription, making IRAK1 activation a key step in the TLR7 and TLR9 signaling cascade[12-19]. Therefore, we examined whether *Pin1* KO affects the ability of IRAK1 to transduce TLR signals.

To address whether IRAK1 is still recruited to the TLR receptor complex in *Pin1* KO cells, we transfected HA-MyD88 into both *Pin1* WT and KO cells retrovirally expressing FLAG-IRAK1, followed by immunoprecipitation with anti-HA antibodies and then immunoblotting with anti-FLAG antibodies. As shown previously[17], the activated form of IRAK1 in *Pin1* WT cells was not readily found in the MyD88 immune complexes **(Fig 5a)**. However, IRAK1 in *Pin1* KO cells formed a stable interaction with HA-MyD88 **(Fig 5a)**, presumably due to the fact that IRAK1 is not fully activated in these cells **(Fig. 4a, 5a)**. Thus it appears that IRAK1 in *Pin1* KO cells is unable to dissociate from the receptor complex due to its lack of autophosphorylation[13, 17], presumably retaining IRAK1 at the receptor complex.

Given that Pin1 is required for IRAK1 activation and dissociation from the receptor complex, we examined whether Pin1 affects IRF7 activation using Pin1 knockdown and knockout. Pin1 knockdown in THP1 monocytes using Pin1-RNAi not only abolished the IRF7 and TRAF6 interaction, as shown by Co-IP experiments **(Fig. 5b)**, but also blocked IRF7 nuclear translocation in response to TLR7 and TLR9 activation, as determined by subcellular fractionation followed by immunoblotting analysis **(Fig. 5c, d)**. To further confirm these results, we immunostained for IRF7 in primary *Pin1* WT and *Pin1* KO pDCs after TLR7 and TLR9 ligation. Upon TLR activation, IRF7 translocated to the nucleus in *Pin1* WT but not *Pin1* KO pDCs **(Fig. 5e)**. These results suggest that Pin1 activates IRAK1 to cause IRF7 nuclear translocation in response to TLR7 or TLR9 stimulation.

This suggestion was further supported by our findings from IRAK1-mediated IRF7 functional assays. Specifically, *Pin1* KO abolished IRF7 reporter activity following TLR7 or TLR9 stimulation **(Fig. 6a, b)**, and these defects were fully rescued by *Pin1*, but not its binding-inactive- or isomerase-defective mutant, as measured by IRF7 reporter activity and IFN-α production **(Fig. 6c, d)**. To further investigate the role of Pin1 and IRAK1 kinase activity in IRF7 activation, we co-expressed MyD88, a Gal4-IRF7 reporter construct and various amounts of KD IRAK1 in Pin1 WT and KO MEFs. IRF7 activation in WT cells decreased as the amount of transfected KD IRAK1 was increased. In contrast, IRF7 activation was consistently lower in *Pin1* KO cells and unaffected by the amount of KD IRAK1 transfected **(Fig. 6e)**. These results demonstrate that both Pin1 and IRAK1 kinase activity are necessary for activation of IRF7. These findings are consistent with the previous findings 1) that IRAK1, but not its KD mutant, phosphorylates IRF7[14], 2) that IRAK1

kinase activity is necessary for the transcriptional activity of IRF7, but not NF-κB[14], 3) that KD IRAK1 inhibits MyD88-induced IRF7 activation in a dominant-negative manner[14], and 4) that inhibition of IRAK kinase activity with a synthetic inhibitor prevents IRF7 phosphorylation, but not NF-κB phosphorylation in CpG stimulated pDCs[33].

IRAK1 mutations that prevented Pin1 binding in retrovirally transfected MEFs including S131A, S144A and S173A alone or together also decreased IRF7 promoter activation and IFN-α secretion similar to kinase-inactivating IRAK1 mutation or Pin1 KO **(Fig. 6f, g)**. To confirm the importance of Pin1 in IRAK1- and IFN-α– mediated antiviral activity, we performed plaque formation assays using GFP-expressing vesicular stomatitis virus (VSV). Specifically, L929 cells were infected with GFP-VSV and incubated with supernatants from Pin1 WT and KO MEFs expressing IRF7 and IRAK1 or its mutants, followed by GFP-positive plaque quantification. While supernatants from Pin1 WT MEFs expressing WT IRAK1 had potent antiviral activity, those from Pin1 WT MEF expressing Pin1 binding IRAK1 mutants or KD IRAK1 had little activity, similar to Pin1 KO MEFs **(Fig. 6h, i)**, consistent with IRF7 activity and IFNα production in these cells **(Fig. 6f, g)**. Thus, disrupting the IRAK1 activation by inhibiting Pin1 or by preventing IRAK1 from acting as a Pin1 substrate drastically abrogates IRF7 activation, subsequent IFN-α production and antiviral response *in vitro*.

Pin1 is required for IRAK1-IRF7-IFN-mediated immunity

Given the essential role for Pin1 on IRAK1-dependent antiviral cellular responses *in vitro*, we next examined the effects of *Pin1* KO *in vivo* using *Pin1* WT and KO mice. Following injection with R-848 or CpG, robust IFN-α production could be observed in *Pin1* WT mice **(Fig. 7a, b)**, as shown[14]. In contrast, serum IFN-α concentrations in *Pin1* KO littermates were reduced **(Fig. 7a, b)**. When injecting mice with LPS or R-848, the serum concentrations of IL-6 and IL-12p40 were lower in *Pin1* KO mice, compared to WT controls, albeit not as dramatically as IFN-α **(Supplementary Fig. 10a-c)**. As the MyD88-IRF7 pathway has been shown to be essential for IFN-α production during MCMV infection[34-37], we next examined the effects of *Pin1* KO on systemic MCMV infection. Whereas IFN-α concentration in *Pin1* WT animals peaked after 36 hours following MCMV infection, IFN-α induction was almost entirely suppressed in *Pin1* KO mice **(Fig. 7c)**. Moreover, Pin1 KO mice were much more vulnerable to systemic MCMV infection than their WT littermates, resulting in increased weight loss **(Fig. 7d)** and morbidity **(Fig. 7e)**. These phenotypes are similar to those observed in *Irf7* or *Myd88* KO mice[34-37] and further highlight the contribution of Pin1 to the antiviral immune response *in vivo*.

Co-stimulation of TLR9 and CD40 induces $CD8^+$ T cell expansion in a pDC, IRF7- and IFN-α-dependent manner, thereby playing a major role in regulation of adaptive immune responses[19, 38]. To study the effects of Pin1 deficiency on adaptive immunity, we next investigated the effects of *Pin1* KO on the induction of antigen-specific $CD8^+$ T-cell responses. As reported[19, 38], treatment with ovalbumin and anti-CD40 alone did not induce specific $CD8^+$ T cell expansion, whereas co-inoculation of CpG-A complexed to DOTAP, a CD40 agonistic antibody and ovalbumin induced a strong expansion of antigen-specific

$CD8^+$ T cells in *Pin1* WT mice **(Fig. 7f, left)**. In contrast, the ovalbumin-specific $CD8^+$ T-cell response was greatly impaired in *Pin1* KO mice **(Fig. 7f, right)**.

These results together indicate that Pin1 is essential for IRAK1 activation in response to TLR7 and TLR9 stimulation. Upon activation, Pin1 activity is upregulated and IRAK1 is autophosphorylated in the UD, allowing Pin1 to bind to and isomerize phosphorylated IRAK1. Such Pin1-catalyzed conformational change facilitates the dissociation of IRAK1 from the receptor complex and recruitment of TRAF6, which combines with IRAK1 to activate IRF7 by promoting nuclear translocation for the induction of type I IFNs to mediate innate and adaptive immunity (**Supplementary Fig. 11a)**. Pin1 deficiency specifically prevents IRAK1 activation and release from the receptor complex, preventing TRAF6 recruitment and IRF7 activation, leading to loss of type I IFN production and its mediated innate and adaptive immunity **(Supplementary Fig. 11b)**.

Discussion

TLRs play an integral role in host defense against a broad range of microorganisms[1-3], with TLR7 and TLR9 being particularly important components of the antiviral machinery[4-7]. IRAK1 has been shown to be essential for TLR7 and TLR9 mediated IFN-α induction[12-14]. However, the mechanisms underlying IRAK1 activation and regulation are not well understood. Our results demonstrate for the first time that Pin1 is a regulator of IRAK1, playing an essential role in TLR signaling and type I IFN-mediated innate and adaptive immunity. Given the major role of aberrant IRAK1 activation and type I IFN overproduction in various immune diseases[10, 11], these results suggest that Pin1 inhibitors, which are under active development[21, 25], may offer a useful therapeutic approach.

We found that Pin1 activity was increased during TLR signaling and that *Pin1* genetic deletion modestly inhibited TLR7- and TLR9-dependent, proinflammatory cytokine production in mDCs, but completely abrogated type I IFN production from pDCs. Consistent with these phenotypes, Pin1 specifically acted on IRAK1 autophosphorylation sites in a TLR-dependent manner. Mechanistic evaluation of the consequences of mutations of the Pin1 binding and isomerizing sites in IRAK1 or genetic deletion of *Pin1* demonstrated that the role of these phosphorylation sites is to promote a conformational change, leading to IRAK1 activation. Such Pin1-catalyzed conformational change facilitates the dissociation of IRAK1 from the receptor complex to activate downstream transcription factors for the induction of type I interferon. Specifically, *Pin1* KO did not affect proximal IRAK1 signaling as its recruitment to the TLR complex and IRAK4 activation were normal. Furthermore, *Pin1* KO did not affect other TLR activated kinases such as the MAPKs. However, *Pin1* KO prevented IRAK1 activation and release from the receptor complex, leading to loss of recruitment of TRAF6 to the complex, resulting in failure of nuclear translocation of IRF7. As a result, *Pin1*-deficient cells and mice failed to mount a robust systemic type I IFN response following R-848 and CpG treatment or MCMV inoculation and became highly susceptible to viral infection. These results demonstrate an essential role for Pin1 in IFN-α mediated innate immunity.

In addition to their central role in innate immunity, TLRs have profound effects on the ensuing adaptive immune response. Type I IFNs not only limit viral replication, but also exert various immunoregulatory effects such as B and T cell activation[39] as well as mDC maturation[40]. Importantly, type I IFNs, following viral infection, also enable cross-priming of $CD8^+$ T cells, thereby allowing the presentation of exogenous antigens in the context of major histocompatability complex (MHC) class I molecules[38]. *Pin1* KO mice were severely defective in triggering an antigen specific $CD8^+$ T-cell response. These results demonstrate the critical role for Pin1 in regulating IRAK1, thereby representing an important new mechanism pivotally positioned at the interface of innate and adaptive immunity.

The tight regulation of IRAK1 is likely required to avoid inflammatory disease. For example, IRAK1 genetic changes are associated with pathological conditions such as SLE, leading to speculation that its increased expression or constitutive activation makes IRAK1 a disease susceptibility factor for IFN-driven autoimmune disorders[41]. Similarly, elevated type I IFN production has been intimately linked to many autoimmune diseases[10, 11, 42].

In particular, aberrant type I IFN signaling now has a firmly demonstrated role in increased susceptibility to various viral infections, autoimmune disease and cancer. Important unifying themes of such diseases are the lack of treatments and the rather unusual prevalence of these diseases in females. For example, women progress to AIDS much faster than men who have the same viral load and this has been at least in part attributed to substantial sex differences in IFN-α secretion arising from HIV-1 stimulation of TLR7 in dendritic cells, which drives increased CD8 T cell activity[43]. Furthermore, the TLR-IRAK1-IRF7-Type I IFN pathway as a key contributor in systemic lupus erythematosus (SLE) pathogenesis, a disease that is particularly prominent in females[44, 45]. Specifically, in SLE patients increased concentrations of antibodies to self antigens such as nucleic acids activate TLRs to drive type I IFNs, which then perpetrate autoimmune tissue destruction and pathogenesis[46]. Furthermore, recent genetic evidence has definitively associated components of the TLR-IRAK-IRF pathway with SLE[47]. A single nucleotide polymorphism in IRAK1 has been associated with increased susceptibility to SLE and *Irak1* KO effectively suppresses SLE in animal models[41]. These examples highlight the important role of IRAK1 and type I IFN in a range of diseases.

One of the challenges arising from the recent wealth of knowledge on TLR signaling is how to develop a strategy to inhibit specific arms of TLR-mediated immune regulation while leaving other critical defensive nodes untouched, a question no doubt asked by many biologists but one rarely answered. The data here reveal that Pin1 inhibition completely abrogates activation of IRAK1 kinase, and fully suppresses type I IFN production, but with only a moderate effects on pro-inflammatory cytokine production. These results suggest that inhibiting either Pin1 and/or IRAK1 kinase activity might allow pharmacological discrimination, which would allow selective inhibition of the type I IFN response while leaving proinflammatory cytokine production unaffected. Such a pharmacological approach might have advantages over conventional immunosuppressing strategies.

Supplementary Material

Refer to Web version on PubMed Central for supplementary material.

Acknowledgements

We thank Lewis Cantley and Tony Hunter for constructive advice and critical reading of the manuscript, and Laurent Brossay, Raymond Welsh, John D Hamilton and Sean Whelan for the viruses. A.T.K. is a fellow of the Swiss Foundation for grants in Biology and Medicine. The work was supported by NIH grants AG029385 to L.K.N. and K.P.L., DK066917 to M.A.E, and GM058556, American Asthma Foundation Senior Investigator Award and Target Identification in Lupus Grant from Alliance for Lupus Research to K.P.L.

Methods

Mice

Pin1 knockout mice have been backcrossed to C57L/B6 for 15 generations to obtain a pure genetic background, with *Pin1*$^{-/-}$ and *Pin1*$^{+}$ littermates being used in all experiments[48].

Preparation of dendritic cells and cytokine measurement

To prepare bone-marrow derived pDC, bone marrow cells were cultured with 100 ng/ml Flt3L (Peprotech) for 6 days. For mDC generation, bone marrow cells were cultured in the presence of 10 ng/ml GM-CSF (PeproTech) for 6 days. Splenic B220^{+}CD11c^{+} pDC were sorted using a LSR II flow cytometer (BD Biosciences). IL-6, IL-12 p40, TNF-α in mDC supernatants following stimulation with the indicated ligands (all from Invivogen) were measured by ELISA (eBioscience). IFN-α in pDC following stimulation with R-848, CpG-A, MCMV (MOI=1) or influenza A virus A/PR/8/34 (H1N1) (MOI=1) was measured by ELISA (PBL InterferonSource) after 24 h.

Quantitative real-time RT–PCR

PDCs were stimulated for 6 h with R-848 or CpG-A and then subjected to quantitative real-time PCR analysis using RotorGene and SYBR Green (Qiagen). Data were normalized to the level of GAPDH expression in each sample. Primers for β-actin, IFN-α1 and IFN-β have previously been described[19].

Pin1 enzymatic activity assay

The Pin1 PPIase assay was performed as previously described[22].

Flow cytometric analysis of cell populations and cytospins

Frequencies of B^{+} cells (CD19^{+},CD3^{-}), CD4^{+} T cells (CD19^{-}CD3^{+}CD4^{+}CD8^{-}), CD8^{+} T cells (CD19^{-}CD3^{+}CD4^{-}CD8^{+}), myeloid DC (MHC-II^{+}CD11c^{+}) and pDC (MHC-II^{+}B220^{+}) were determined by staining with the corresponding antibodies (eBioscience). Cells were analyzed using a LSR II flow cytometer (BD Biosciences) and FlowJo software.

For cytospins, pDCs were spun onto glass slides, air dried, fixed in methanol and thereafter stained with an anti-IRF7 antibody (Abcam), followed by an Alexa Fluor 488 conjugated secondary antibody. Slides were counterstained with DAPI.

GST-Pin1 pull down, immunoprecipitation, and immunoblotting analyses

GST pulldown, immunoprecipitation, and immunoblotting analyses were performed as described[28]. Antibodies against IRAK1, IRAK4, IκBα, IRF7, p-ERK, p-JNK, p-p38, and lamin antibodies were from Cell Signaling. In some experiments an IRAK1 antibody from Millipore was used. TRAF6 antibodies were from Santa Cruz, Tubulin antibody was from Sigma. MyD88 antibody was from Stressgen. Anti-Pin1 monoclonal antibody was made as described[48].

Far-Western blotting analysis

Far-Western analysis was performed as described[22] .

Tandem Mass Spectrometry

Coomassie-stained SDS-PAGE gel bands were excised, reduced with DTT, alkylation with iodoacetamide followed by in-gel digestion with trypsin overnight. Reversed-phase microcapillary liquid chromatography tandem mass spectrometry (LC-MS/MS) was performed..

Phosphorylated Ser173-specific IRAK1 antibodies

Phosphorylated Ser173-specific IRAK1 antibodies were raised by immunizing rabbits with a KLH-coupled phosphorylated Ser173-containing IRAK1 peptide (Proteintech Group) and were affinity purified, as described[48].

NMR spectroscopy

Recombinant Pin1 and its WW domain were expressed as N-terminal GST or His fusion proteins, followed by thrombin cut to remove the tag[31]. NMR experiments were performed at a temperature of 25°C on a Varian Inova 600 MHz spectrometer equipped with a (H,C,N) Z-axis gradient probe, as described[32]. Spectra were processed and analyzed using the software tools nmrPipe, nmrDraw and Sparky.

Generation of stable cell lines

For retroviral transduction, viral supernatants were prepared using Phoenix HEK293 cells as per manufacturers instructions (Orbigen). Stable cell pools were checked for protein expression by immunoblotting analysis with various antibodies to confirm protein expression. Stable cell lines were maintained in culture using 1 μg/ml puromycin.

In vitro and in cell kinase assays

In vitro kinase assays were performed as previously described[27].

Cell fractionation

Nuclear and cytosolic fractions were prepared with NE-PER (Pierce), as described previously[49].

Reporter Gene Assays

Pin1^{+} and *Pin1*$^{-/-}$ MEFs stably expressing IRAK1 and its mutants in 24-well plates were transfected with Gal4-IRF7 and 40 ng of the $UAS_{(GAL)}$-luciferase reporter gene using Lipofectamine 2000 (Invitrogen), as described previously[49]. In some experiments, cells were simultaneously transfected with constructs for Myd88 (20 ng), Pin1 WT, Pin1 W34A and Pin1 K63A (each 100 ng/well) or TLR7 and TLR9 (each 10 ng/well). Renilla luciferase reporter gene (50 ng) was co-transfected as an internal control.

Measurement of IFN-α production in stable cell lines and mice

MEFs stably expressing IRAK1 and its mutants or empty vector were transiently transfected with mIRF7 (20 ng/well) (Invivogen) in 24-well plates. In some experiments, cells were co-transfected with Pin1 WT, Pin1 W34A or Pin1 K63A (100 ng/well). IFN-α concentrations in the supernatants were measured by ELISA after 24 h. To measure serum IFN-α levels by ELISA, mice were intravenously injected with R-848 (50 nmol), CpG-A (5 μg) complexed to DOTAP (Roche) or intraperitoneally with MCMV (10^5 PFU). Blood was drawn from the tail vein at various time points.

Plaque assays

L929 cells cultured in 6 well plates were incubated over night with culture supernatants of MEFs stably expressing IRAK1 and its mutants or empty vector. L929 cells were then infected with VSV-GFP (a kind of Dr. Sean Whelan, Harvard Medical School) at a multiplicity of infection (MOI) of 0.02 for 4 h. Medium was then removed and the corresponding cell culture supernatants containing 0.5% agarose were added to each well. GFP positive plaques were counted after 24 h using a fluorescence microscope.

Susceptibility to MCMV infection

To assess the effect of MCMV infection on body weight, mice (n=6) were injected i.p. with 2.5×10^4 PFU of the salivary gland derived MCMV clone RVG-102 (MCMV-GFP) (kindly provided by Dr. Laurent Brossay, Brown University) which is recombinant for GFP under the immediate-early gene 1 (Ie-1) promoter and has acute and latent infection characteristics similar to those of wild-type MCMV[50]. To measure MCMV-mediated morbidity, mice were i.p. injected with 10^5 PFU. Mice were sacrificed once they reached a moribund state. All experiments were performed according to a protocol approved by the Beth Israel Deaconess IACUC.

Antigen-specific CD8+ T-cell expansion

Expansion of ovalbumin-specific $CD8^+$ T cells was measured using a MHC class I tetramer[38]. Briefly, mice were injected i.p with 30 μg CpG-A complexed to DOTAP, 50 μg anti-CD40 (clone FGK45; Alexis) and 0.5 mg ovalbumin (Sigma-Aldrich). After 6 d, ova-specific splenic CD 8^+ T cells were detected with CD8a-APC and CD44-FITC antibodies and a PE-conjugated H-$2K^b$ tetramer containing the SIINFEKL peptide. Cells were analyzed using a flow cytometer. Results are representative of 3 independent experiments.

References

1. O'Neill LA. The interleukin-1 receptor/Toll-like receptor superfamily: 10 years of progress. Immunol Rev. 2008; 226:10–18. [PubMed: 19161412]
2. Takeuchi O, Akira S. Pattern recognition receptors and inflammation. Cell. 2010; 140:805–820. [PubMed: 20303872]
3. Iwasaki A, Medzhitov R. Regulation of adaptive immunity by the innate immune system. Science. 2010; 327:291–295. [PubMed: 20075244]
4. Hemmi H, et al. A Toll-like receptor recognizes bacterial DNA. Nature. 2000; 408:740–745. [PubMed: 11130078]
5. Hemmi H, et al. Small anti-viral compounds activate immune cells via the TLR7 MyD88-dependent signaling pathway. Nat Immunol. 2002; 3:196–200. [PubMed: 11812998]
6. Diebold SS, Kaisho T, Hemmi H, Akira S, Reis e Sousa C. Innate antiviral responses by means of TLR7-mediated recognition of single-stranded RNA. Science. 2004; 303:1529–1531. [PubMed: 14976261]
7. Heil F, et al. Species-specific recognition of single-stranded RNA via toll-like receptor 7 and 8. Science. 2004; 303:1526–1529. [PubMed: 14976262]
8. Liu YJ. IPC: professional type 1 interferon-producing cells and plasmacytoid dendritic cell precursors. Annu Rev Immunol. 2005; 23:275–306. [PubMed: 15771572]
9. Hoebe K, Janssen E, Beutler B. The interface between innate and adaptive immunity. Nat Immunol. 2004; 5:971–974. [PubMed: 15454919]
10. Baccala R, Hoebe K, Kono DH, Beutler B, Theofilopoulos AN. TLR-dependent and TLR-independent pathways of type I interferon induction in systemic autoimmunity. Nat Med. 2007; 13:543–551. [PubMed: 17479100]
11. Banchereau J, Pascual V. Type I interferon in systemic lupus erythematosus and other autoimmune diseases. Immunity. 2006; 25:383–392. [PubMed: 16979570]
12. Cao Z, Henzel WJ, Gao X. IRAK: a kinase associated with the interleukin-1 receptor. Science. 1996; 271:1128–1131. [PubMed: 8599092]
13. Wesche H, Henzel WJ, Shillinglaw W, Li S, Cao Z. MyD88: an adapter that recruits IRAK to the IL-1 receptor complex. Immunity. 1997; 7:837–847. [PubMed: 9430229]
14. Uematsu S, et al. Interleukin-1 receptor-associated kinase-1 plays an essential role for Toll-like receptor (TLR)7- and TLR9-mediated interferon-{alpha} induction. J Exp Med. 2005; 201:915–923. [PubMed: 15767370]
15. Kawai T, et al. Interferon-alpha induction through Toll-like receptors involves a direct interaction of IRF7 with MyD88 and TRAF6. Nat Immunol. 2004; 5:1061–1068. [PubMed: 15361868]
16. Honda K, et al. Role of a transductional-transcriptional processor complex involving MyD88 and IRF-7 in Toll-like receptor signaling. Proc Natl Acad Sci U S A. 2004; 101:15416–15421. [PubMed: 15492225]
17. Kollewe C, et al. Sequential autophosphorylation steps in the interleukin-1 receptor-associated kinase-1 regulate its availability as an adapter in interleukin-1 signaling. J Biol Chem. 2004; 279:5227–5236. [PubMed: 14625308]
18. Honda K, et al. Spatiotemporal regulation of MyD88-IRF-7 signalling for robust type-I interferon induction. Nature. 2005; 434:1035–1040. [PubMed: 15815647]

19. Honda K, et al. IRF-7 is the master regulator of type-I interferon-dependent immune responses. Nature. 2005; 434:772–777. [PubMed: 15800576]
20. Thomas JA, et al. Impaired cytokine signaling in mice lacking the IL-1 receptor-associated kinase. J Immunol. 1999; 163:978–984. [PubMed: 10395695]
21. Lu KP, Zhou XZ. The prolyl isomerase Pin1: a pivotal new twist in phosphorylation signalling and human disease. Nat Rev Mol Cell Biol. 2007; 8:904–916. [PubMed: 17878917]
22. Yaffe MB, et al. Sequence-specific and phosphorylation-dependent proline isomerization: A potential mitotic regulatory mechanism. Science. 1997; 278:1957–1960. [PubMed: 9395400]
23. Saitoh T, et al. Negative regulation of interferon-regulatory factor 3-dependent innate antiviral response by the prolyl isomerase Pin1. Nat Immunol. 2006; 7:598–605. [PubMed: 16699525]
24. Honda K, Taniguchi T. IRFs: master regulators of signalling by Toll-like receptors and cytosolic pattern-recognition receptors. Nat Rev Immunol. 2006; 6:644–658. [PubMed: 16932750]
25. Wildemann D, et al. Nanomolar Inhibitors of the Peptidyl Prolyl Cis/Trans Isomerase Pin1 from Combinatorial Peptide Libraries. J Med Chem. 2006; 49:2147–2150. [PubMed: 16570909]
26. Jewell NA, et al. Differential type I interferon induction by respiratory syncytial virus and influenza a virus in vivo. J Virol. 2007; 81:9790–9800. [PubMed: 17626092]
27. Shen ZJ, Esnault S, Malter JS. The peptidyl-prolyl isomerase Pin1 regulates the stability of granulocyte-macrophage colony-stimulating factor mRNA in activated eosinophils. Nat Immunol. 2005; 6:1280–1287. [PubMed: 16273101]
28. Lu PJ, Zhou XZ, Shen M, Lu KP. A function of WW domains as phosphoserine- or phosphothreonine-binding modules. Science. 1999; 283:1325–1328. [PubMed: 10037602]
29. Hoshino K, et al. Critical role of IkappaB Kinase alpha in TLR7/9-induced type I IFN production by conventional dendritic cells. J Immunol. 2010; 184:3341–3345. [PubMed: 20200270]
30. Li X, et al. Mutant cells that do not respond to interleukin-1 (IL-1) reveal a novel role for IL-1 receptor-associated kinase. Mol Cell Biol. 1999; 19:4643–4652. [PubMed: 10373513]
31. Ranganathan R, Lu KP, Hunter T, Noel JP. Structural and functional analysis of the mitotic peptidyl-prolyl isomerase Pin1 suggests that substrate recognition is phosphorylation dependent. Cell. 1997; 89:875–886. [PubMed: 9200606]
32. Pastorino L, et al. The prolyl isomerase Pin1 regulates amyloid precursor protein processing and amyloid-beta production. Nature. 2006; 440:528–534. [PubMed: 16554819]
33. Chiang EY, Yu X, Grogan JL. Immune complex-mediated cell activation from systemic lupus erythematosus and rheumatoid arthritis patients elaborate different requirements for IRAK1/4 kinase activity across human cell types. J Immunol. 2011; 186:1279–1288. [PubMed: 21160042]
34. Krug A, et al. TLR9-dependent recognition of MCMV by IPC and DC generates coordinated cytokine responses that activate antiviral NK cell function. Immunity. 2004; 21:107–119. [PubMed: 15345224]
35. Dalod M, et al. Interferon alpha/beta and interleukin 12 responses to viral infections: pathways regulating dendritic cell cytokine expression in vivo. J Exp Med. 2002; 195:517–528. [PubMed: 11854364]
36. Delale T, et al. MyD88-dependent and -independent murine cytomegalovirus sensing for IFN-alpha release and initiation of immune responses in vivo. J Immunol. 2005; 175:6723–6732. [PubMed: 16272328]
37. Steinberg C, et al. The IFN regulatory factor 7-dependent type I IFN response is not essential for early resistance against murine cytomegalovirus infection. Eur J Immunol. 2009; 39:1007–1018. [PubMed: 19283778]
38. Ahonen CL, et al. Combined TLR and CD40 triggering induces potent CD8+ T cell expansion with variable dependence on type I IFN. J Exp Med. 2004; 199:775–784. [PubMed: 15007094]
39. Nguyen KB, et al. Critical role for STAT4 activation by type 1 interferons in the interferon-gamma response to viral infection. Science. 2002; 297:2063–2066. [PubMed: 12242445]
40. Honda K, et al. Selective contribution of IFN-alpha/beta signaling to the maturation of dendritic cells induced by double-stranded RNA or viral infection. Proc Natl Acad Sci U S A. 2003; 100:10872–10877. [PubMed: 12960379]

41. Jacob CO, et al. Identification of IRAK1 as a risk gene with critical role in the pathogenesis of systemic lupus erythematosus. Proc Natl Acad Sci U S A. 2009; 106:6256–6261. [PubMed: 19329491]
42. Theofilopoulos AN, Baccala R, Beutler B, Kono DH. Type I interferons (alpha/beta) in immunity and autoimmunity. Annu Rev Immunol. 2005; 23:307–336. [PubMed: 15771573]
43. Meier A, et al. Sex differences in the Toll-like receptor-mediated response of plasmacytoid dendritic cells to HIV-1. Nat Med. 2009; 15:955–959. [PubMed: 19597505]
44. Trinchieri G. Type I interferon: friend or foe? J Exp Med. 2010; 207:2053–2063. [PubMed: 20837696]
45. Rahman AH, Eisenberg RA. The role of toll-like receptors in systemic lupus erythematosus. Springer Semin Immunopathol. 2006; 28:131–143. [PubMed: 17047954]
46. Rahman A, Isenberg DA. Systemic lupus erythematosus. N Engl J Med. 2008; 358:929–939. [PubMed: 18305268]
47. Gateva V, et al. A large-scale replication study identifies TNIP1, PRDM1, JAZF1, UHRF1BP1 and IL10 as risk loci for systemic lupus erythematosus. Nat Genet. 2009; 41:1228–1233. [PubMed: 19838195]
48. Lee TH, et al. Essential role of Pin1 in the regulation of TRF1 stability and telomere maintenance. Nat Cell Biol. 2009; 11:97–105. [PubMed: 19060891]
49. Ryo A, et al. Regulation of NF-kappaB signaling by Pin1-dependent prolyl isomerization and ubiquitin-mediated proteolysis of p65/RelA. Mol Cell. 2003; 12:1413–1426. [PubMed: 14690596]
50. Henry SC, et al. Enhanced green fluorescent protein as a marker for localizing murine cytomegalovirus in acute and latent infection. J Virol Methods. 2000; 89:61–73. [PubMed: 10996640]

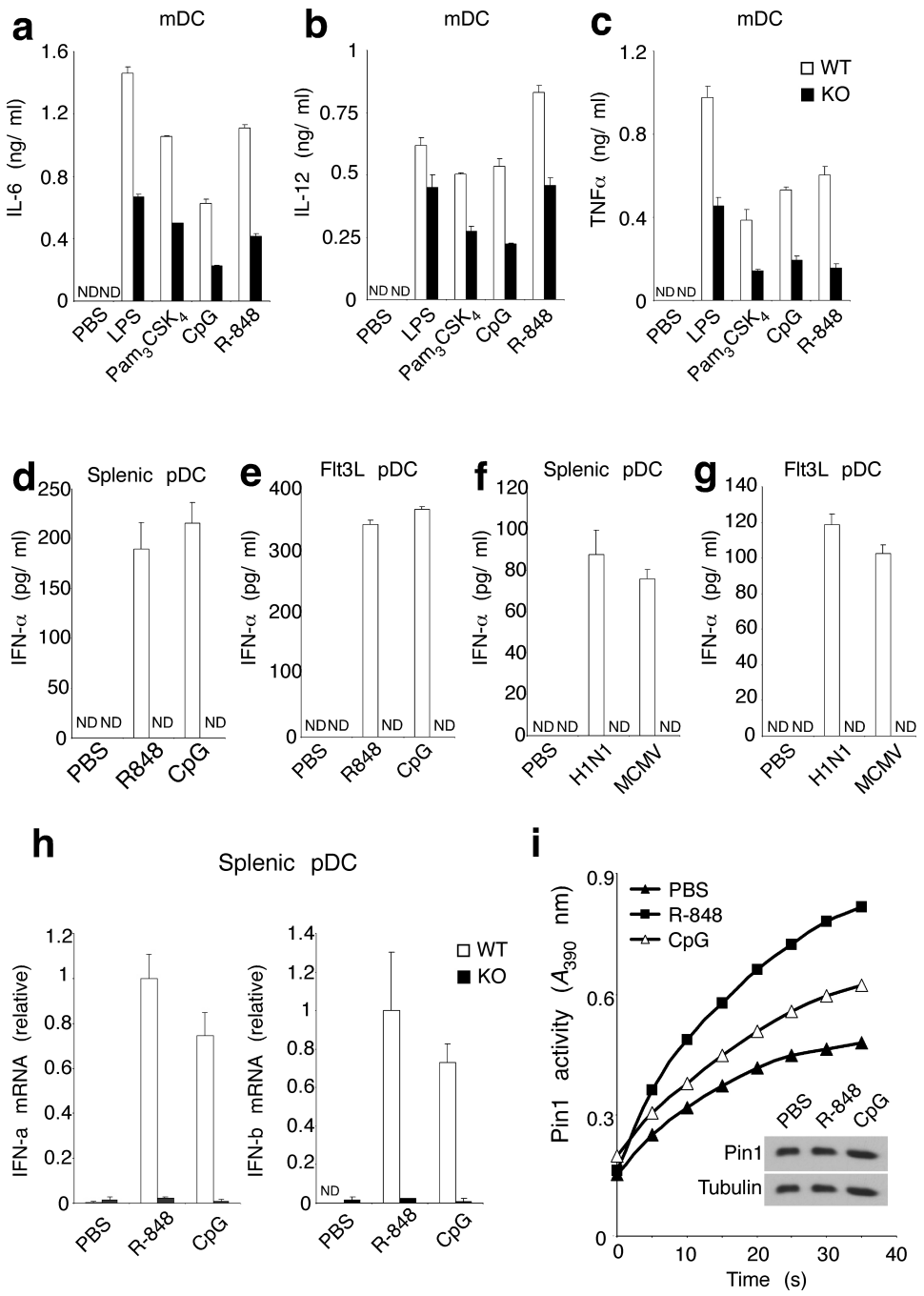

Figure 1. Pin1 is activated and required for cytokine and especially type I IFN secretion following TLR stimulation

(**a-c)** Impaired TLR7- and TLR9-induced cytokine production from *Pin1* KO mDCs. Bone-marrow-derived mDCs were stimulated with 100 ng/ml LPS, 1 μg/ml Pam3CSK4, 0.1 μg/ml R-848 or 0.1 μM CpG-B. Concentrations of IL-6 (**a**), IL-12p40 (**b**), TNF (**c**) measured in cell-culture supernatants after 12 h are shown.

(**d, e)** IFN-α concentration in supernatants after R-848 and CpG-A treatment of purified splenic pDCs ($B220^{+}CD11c^{int}$) (**d**) and Flt3L-induced bone-marrow-derived pDCs for 24 h (**e**).

(**f, g)** IFN-α levels in supernatants following stimulation of splenic (**f**) and Flt3L-induced bone-marrow-derived pDCs (**g**) for 24 h with Influenza A (H1N1) virus or MCMV. IFN-α concentrations were measured by ELISA. Bars indicate means ±s.d. of triplicate determinations.

(**h**) Splenic pDCs were stimulated with PBS, R-848 or CpG DNA for 6 h. Expression of IFN-α or β mRNAs was measured by quantitative real-time RT–PCR analysis. Data were normalized to the levels of *Gapdh* expression. Results shown are means ± s.d. of triplicates.

(**i**) Pin1 catalytic activity, but not protein level, is increased upon TLR7 or TLR9 stimulation. Purified human PBMC were treated for 30 min either with PBS (▲), R-848 (■) or CpG DNA (△) and lysed, followed by protease-coupled isomerase activity assay for Pin1 activity. Results are representative of 3 independent experiments. Following the Pin1 protease coupled isomerase activity assay, fractions of lysates were subjected to immunoblotting analysis using Pin1 antibody with tubulin as a control **(inset)**.

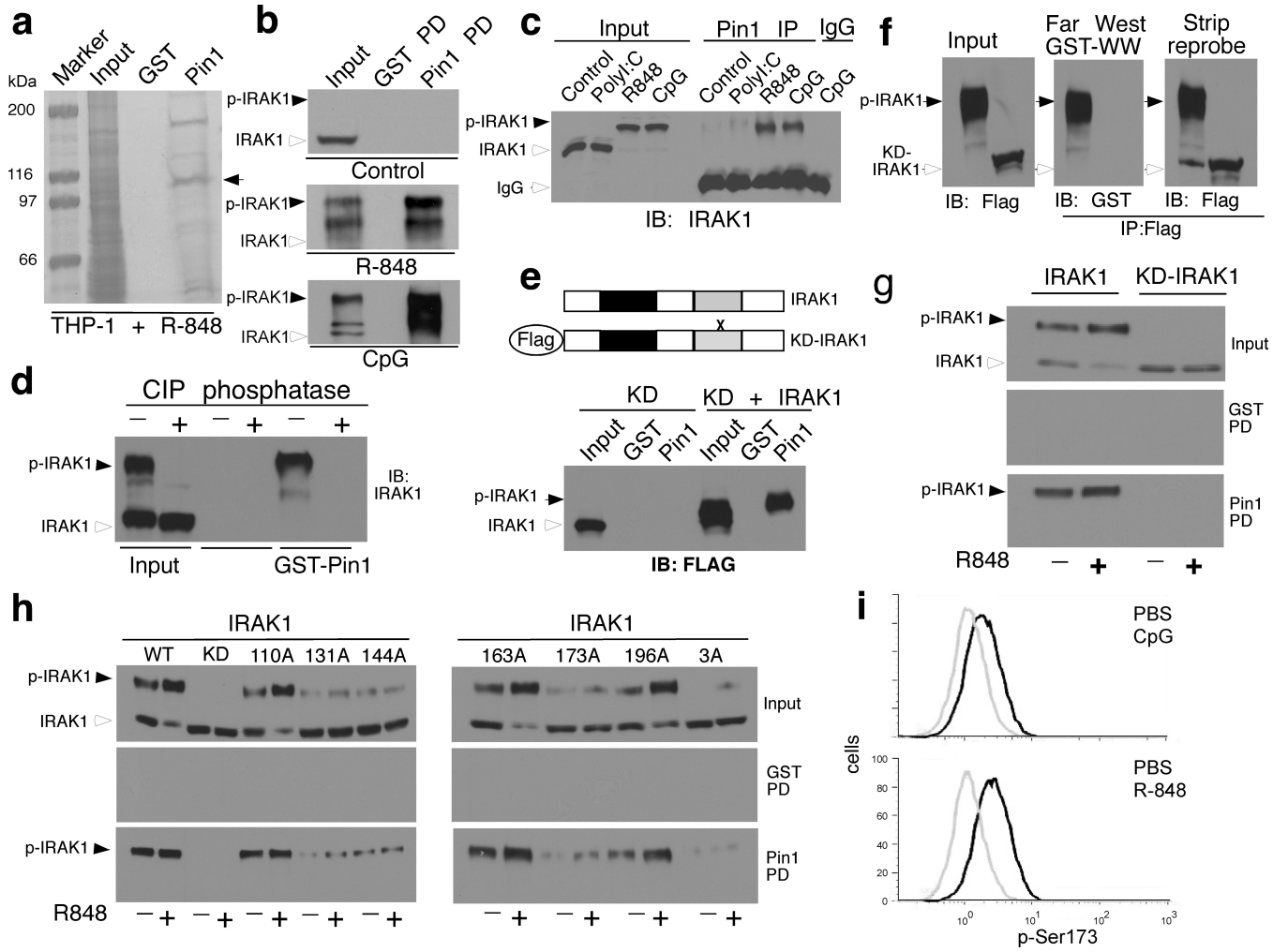

Figure 2. Proteomic approach identifies IRAK1 as a major Pin1 substrate upon TLR stimulation

(a) Proteomic identification of IRAK1 as a TLR-induced Pin1 binding protein. THP1 cells stimulated with R-848 for 45 min were lysed and subjected to GST-Pin1 pulldown followed by SDS-PAGE and colloidal CBB staining. Specific GST-Pin1 interacting bands were excised and 7 peptides were identified to IRAK1 by LC-MS **(Supplementary Fig. 3a)**.

(b) TLR-dependent interaction between Pin1 and IRAK1, assayed by GST-Pin1 pulldown. RAW264.7 cells stimulated with PBS or either R-848 or CpG for 30 min were subjected to immunoblotting analysis using IRAK1 antibodies after pulldown with GST or GST-Pin1.

(c) TLR-dependent interaction between endogenous Pin1 and IRAK1, assayed by Co-IP. THP1 cells were stimulated with poly(I:C), R-848 or CpG and subjected to immunoprecipitation with anti-Pin1 antibodies or control IgG, followed by immunoblotting with IRAK1 antibodies.

(d) The IRAK1-Pin1 interaction is sensitive to phosphatase treatment. TLR7-HEK293T cells were transfected with FLAG-IRAK1 and stimulated with R-848 and lysates were untreated or treated with calf intestinal phosphatase (CIP) phosphatase for 60 min at 30°C, followed by GST-Pin1 pulldown experiments.

(e) The Pin1-IRAK1 interaction is dependent on the intrinsic kinase activity of IRAK1. FLAG-KD-IRAK1, either alone or in combination with IRAK1 were expressed in IRAK1-deficient 293T cells, followed by GST pulldown experiments

(f) Pin1 binds directly to phosphorylated WT IRAK1, but not KD IRAK1. FLAG-IRAK1 and FLAG-KD IRAK1 were expressed in IRAK1-deficient 293T cells and purified using FLAG-agarose, followed by Far-Western analysis using GST-Pin1 WW domain to detect Pin1 binding using anti-GST antibody. Membranes were re-probed with FLAG antibody as a control.

(g) Pin1 binds to activated WT IRAK1, but not KD IRAK1 in MEFs. FLAG-IRAK1 and its KD mutant were expressed in MEFs using retroviral infection and then treated with R-848 or control buffer, followed by GST pulldown experiments.

(h) Multiple pSer-Pro motifs in the undetermined domain (UD) of IRAK1 are required for Pin1 binding. FLAG-IRAK1 and its mutants were expressed in MEFs using retroviral infection, and then treated with R-848 or control buffer, followed by GST pulldown experiments.

(**i**) S173 phosphorylation of IRAK1 is induced upon TLR7 and TLR9 stimulation. THP1 cells were stimuylated with CpG or R-848 and thereafter intracellularly stained with an anti-pS173 antibody, followed by a secondary FITC conjugated antibody. Fluorescence was measured by flow cytometry.

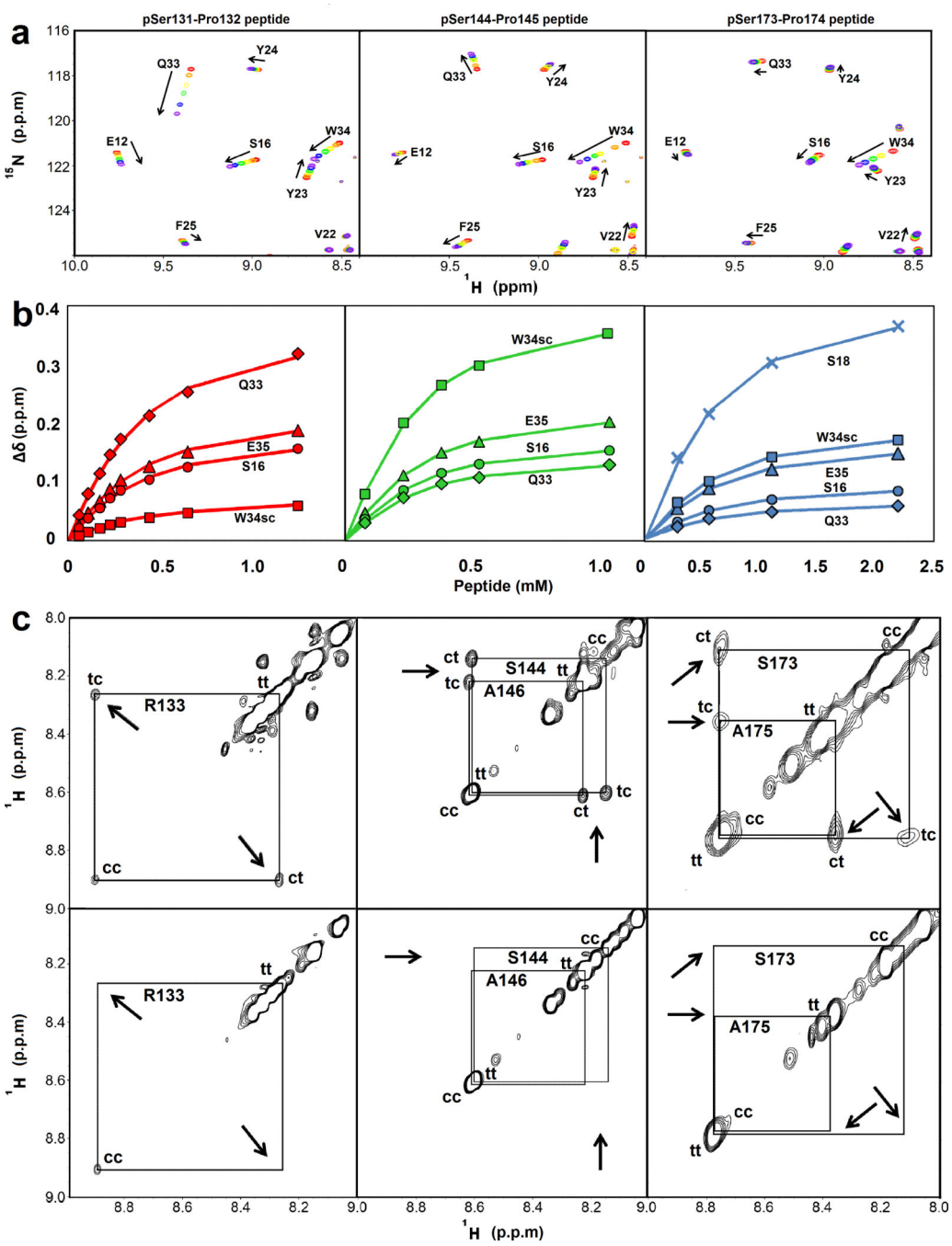

Figure 3. Phosphorylated S131-, S144- and S173-Pro sites in the IRAK-1 UD bind to and are isomerized by Pin1

(a) Representative chemical shift perturbations in ^{15}N-WW detected using 2D ^{15}N-^{1}H HSQC spectra resulting from titration with IRAK-1 peptides phosphorylated at Ser131, Ser144, and Ser173. Apo peaks are shown in red, and sequential colors represent increasing concentrations of peptides, purple being highest.

(b) Representative binding curves for WW domain residues, showing weighted chemical shift changes ($\Delta\delta = \mathrm{sqrt}[\Delta\delta_{1H}^2 + (0.154\Delta\delta_{15N}^2]$) as a function of total concentration of

peptide. Residues plotted are S16 (●), S18 (×), Q33 (◆), the sidechain of W34 (■), and E35 (▲). Lines represent global fits.

(**c**) 2D ^{1}H-^{1}H ROESY spectra (mixing time of 100 ms) of IRAK-1 phosphopeptides in the presence (top panels) or absence (bottom panels) of a catalytic amount of Pin1. The appearance of exchange crosspeaks (arrows) between peaks corresponding to the cis and trans isomers confirms that Pin1 acts catalytically on these sequences.

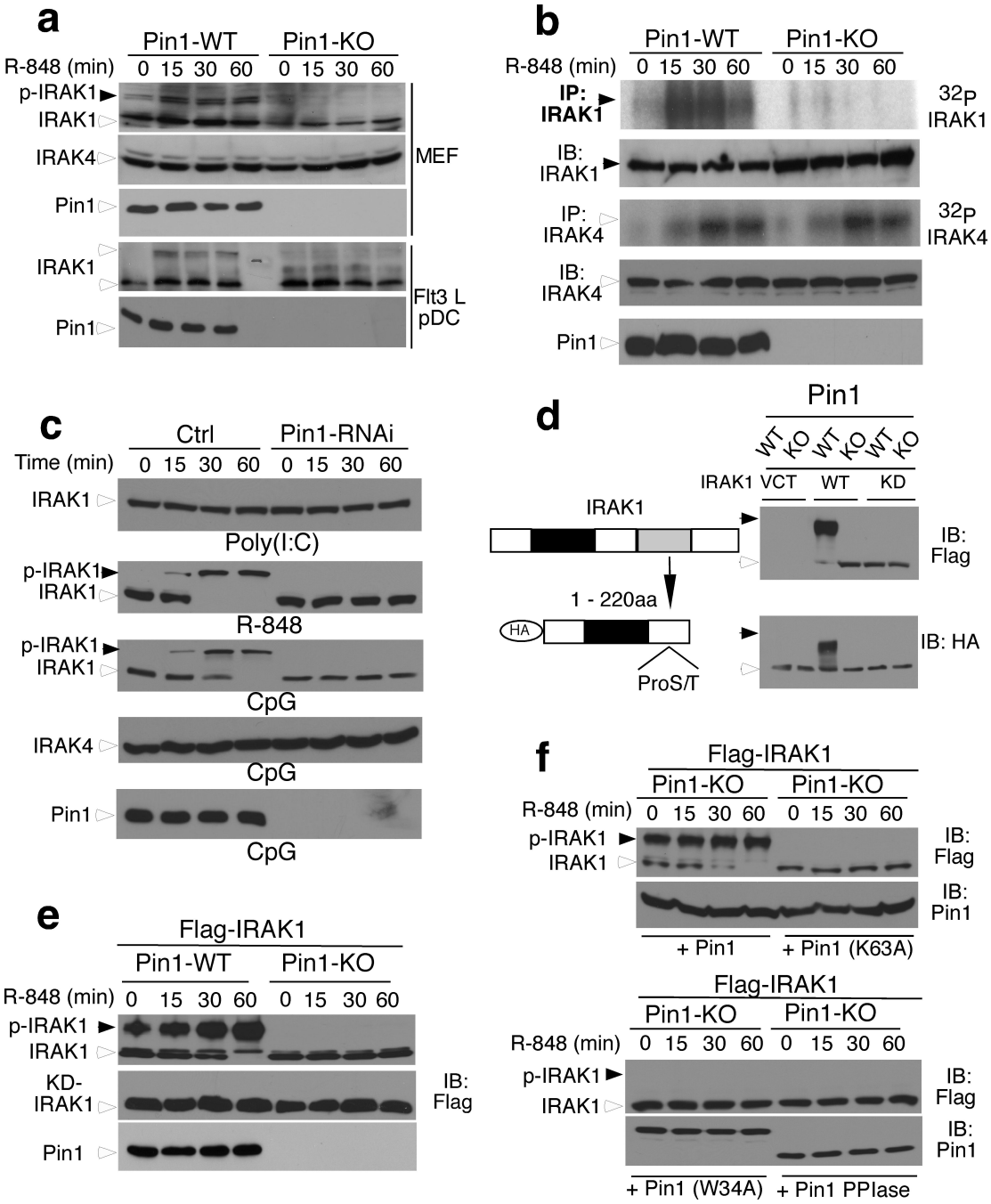

Figure 4. Pin1 is essential for IRAK1 activation upon TLR ligation

(a) *Pin1* KO completely blocks IRAK1 activation in mouse cells following TLR7 stimulation. *Pin1* WT and KO Flt3-derived pDCs (bottom) or TLR7-expressing MEF cells (top) were simulated with R-848 for the indicated times and analyzed for the characteristic IRAK1 shift by immunoblotting with IRAK1 antibodies, with IRAK4 and Pin1 amounts as controls.

(b) *Pin1* KO completely blocks activation of IRAK1, but not IRAK4 following TLR7 stimulation. Peritoneal macrophages from *Pin1* WT and KO mice were stimulated with

R-848 for the indicated times and kinase activity of IRAK1 and IRAK4 was assessed by an IP kinase autophosphorylation assay. IRAK1, IRAK4 and Pin1 protein were assayed as controls. **(c)** *Pin1* knockdown blocks IRAK1 activation in human cells following TLR7 and TLR9, but not TLR3 stimulation. Human THP1 monocytes were infected with viral control shRNA or shRNA targeting Pin1 and simulated with poly (I:C) (TLR3), R-848 or CpG ligands for the indicated times, followed by analyzing the characteristic IRAK1 shift using immunoblotting.

(d) *In vivo* kinase assay demonstrates IRAK1 kinase activity in *Pin1* WT, but not *Pin1* KO cells. Retroviral FLAG-IRAK1, and KD-IRAK1 or vector (VCT) control were coexpressed with a HA-N-terminal 220 aa fragment of IRAK1 as a substrate in *Pin1* WT and KO MEFs (schematic diagram). IRAK1 kinase activity was determined by immunoblotting with HA antibodies to assess the characteristic mobility shift in IRAK1 N-terminal 220 aa due to trans-phosphorylation by co-expressed IRAK1 proteins.

(e) *Pin1* KO abolishes TLR dependent activation of exogenous IRAK1 *in vivo*. FLAG-IRAK1 and its KD mutant were co-expressed with TLR7 in *Pin1* WT and KO MEF cells using retroviral vectors and stimulated with R-848 for the indicated times, followed by analyzing the characteristic IRAK1 mobility shift using immunoblotting.

(f) Pin1, but not its WW domain-binding mutant (W34A) or catalytically inactive PPIase domain mutant (K63A), fully rescues IRAK1 activation in *Pin1* KO cells. *Pin1* KO MEFs stably expressing FLAG-IRAK1 were transfected with either WT-Pin1, K63A-Pin1, W34A-Pin1 or PPIase domain of Pin1 and TLR7 and stimulated for the indicated times, followed by analyzing the characteristic IRAK1 mobility shift using immunoblotting. Results are representative of at least three independent experiments.

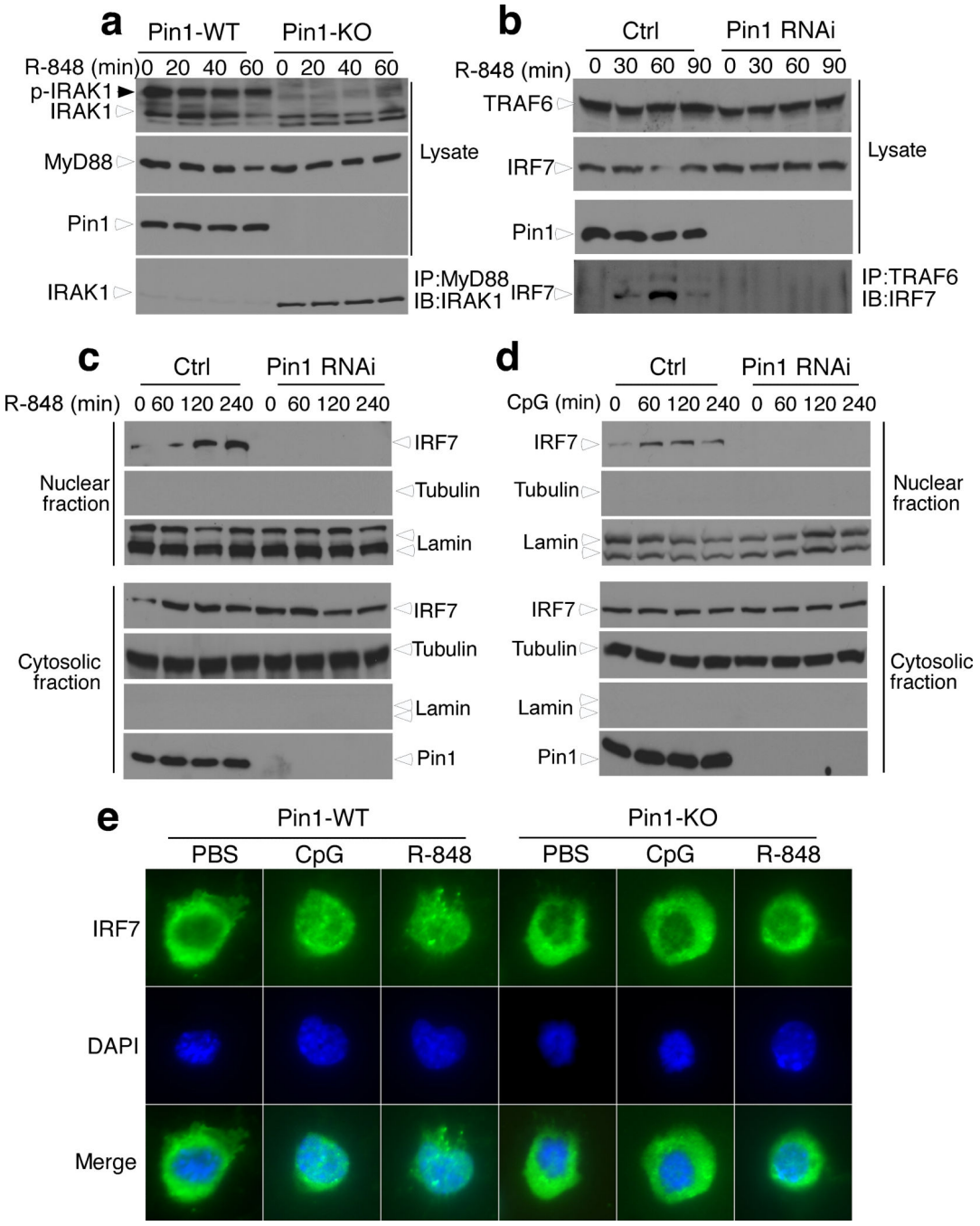

Figure 5. Pin1 facilitates IRAK1 release from the receptor complex to activate IRF7 following TLR ligation

(a) Activated and phosphorylated IRAK1 is released from MyD88 in *Pin1* WT cells, but inactive IRAK1 is not in *Pin1* KO cells. HA-MyD88 and FLAG-IRAK1 were co-expressed in *Pin1* WT and KO MEF using retroviral expression vectors, followed by immunoprecipitation with anti-HA antibody and then immunoblotting with anti-FLAG antibody.

(b) *Pin1* knockdown inhibits the interaction of IRF7 with TRAF6. THP1 cells expressing *Pin1*-RNAi or control RNAi were stimulated with CpG for the indicated times and the interaction of IRF7 and TRAF6 was examined by Co-IP.

(c, d) *Pin1* knockdown prevents IRF7 nuclear translocation in human THP1 cells. Following TLR7 **(c)** or TLR9 **(d)** ligation for the indicated times, nuclear and cytoplasmic fractions of THP1 cells were prepared, followed by immunoblotting with IRF7 antibody. The purity of nuclear and cytosolic fractions was evaluated by immunoblotting with tubulin or lamin A/C antibodies, respectively.

(e) *Pin1* KO prevents IRF7 nuclear translocation after TLR7 or TLR9 ligation in pDCs. After R484 or CpG stimulation, Pin1 WT and KO pDCs were immunostained with IRF7 antibodies and counter-stained with DAPI, followed by confocal microscopy. Results are representative of at least three independent experiments.

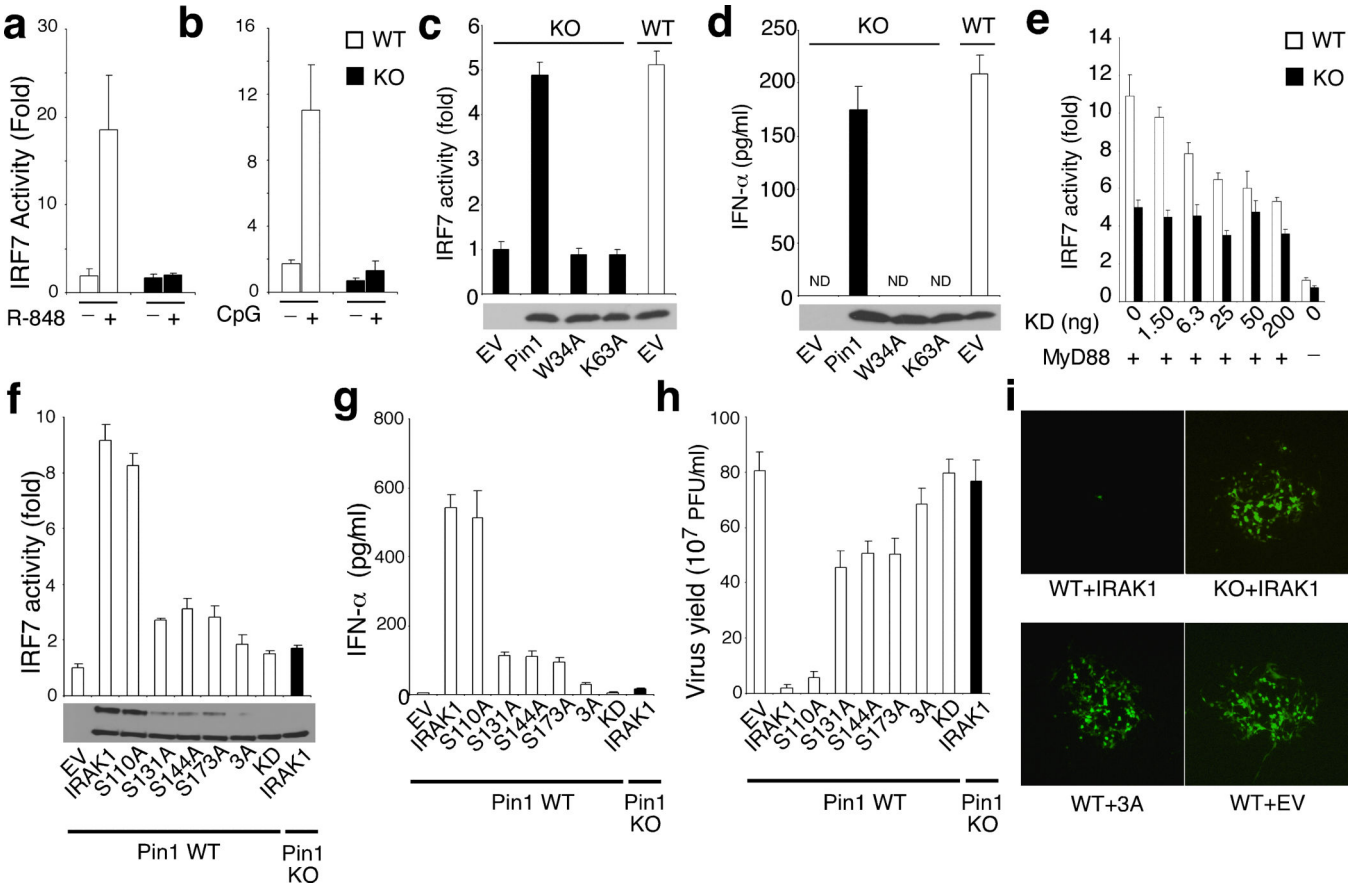

Figure 6. Pin1 is required for IRF7 activation and IFN-α production upon TLR ligation *in vitro*

(a, b) Pin1 is required for IRF7 activation in response to TLR7 or TLR9 activation. Pin1 WT and KO cells transiently co-expressing a $UAS_{(GAL)}$-reporter plasmid, Gal4-IRF7 and TLR7 **(a)** or TLR9 **(b)** were stimulated with R-848 or CpG, respectively, followed by luciferase assay 12 h later using renilla luciferase to normalize for transfection efficiency.

(c, d) Re-expression of Pin1, but not its mutants, fully rescues impaired IRF7 activation and IFN-α production in *Pin1* KO cells. *Pin1* WT and KO MEFs stably expressing IRAK1 were transiently co-transfected with $UAS_{(GAL)}$ and Gal4-IRF7 and empty vector (EV), Pin1, WW domain mutant (W34A) or PPIase domain mutant (K63A), followed by luciferase assay **(c)** and IFN-α ELISA **(d)**, with *Pin1* WT MEFs stably expressing IRAK1 transfected with EV as a control. Expression levels of WT, W34A and K63A Pin1 proteins are shown below graphs in **(c)** and **(d)**.

(e) Overexpression of KD IRAK1 inhibits IRF7 activity in *Pin1* WT, but does not affect basal IRF7 activity in Pin1 KO MEFs. *Pin1* WT and KO MEFs were transiently transfected with Gal4-IRF7, $UAS_{(Gal)}$, MyD88 (20 ng) and various amounts of KD *Irak1* or control vector, as indicated, followed by assaying IRF7 activity using Renilla as a control for normalization.

(f, g) *Pin1* KO or IRAK1 mutations that prevent IRAK1 from being a Pin1 substrate abolish IRF7 activation and IFN-α production. *Pin1* WT and KO cells stably expressing empty vector (EV), IRAK1 or IRAK1 mutants S110A, S131, S144, S173A, 3A (S131+S144+S173A) or KD were co-transfected with $UAS_{(GAL)}$ and Gal4-IRF7 to assess

IRF7 reporter activity **(f)** or with IRF7 to measure IFN-α production **(g)**. Expression levels of IRAK1 and its various mutants are shown below the graph **(f)**.

(h, i) *Pin1* KO or *Irak1* mutations that prevent IRAK1 from being a Pin1 substrate abolish antiviral activity. VSV production in plaque-forming units (PFU) per ml 24 h after infection of monolayer L cells (0.1 PFU/cell) previously treated with supernatants from *Pin1* WT and KO cells stably expressing EV, IRAK1 or IRAK1 mutants S110A, S131, S144, S173A, 3A or KD **(h)**, with representative pictures of VSV plaques shown in **(i)**. ND, not detectable. Results shown are means ± s.d. of triplicates.

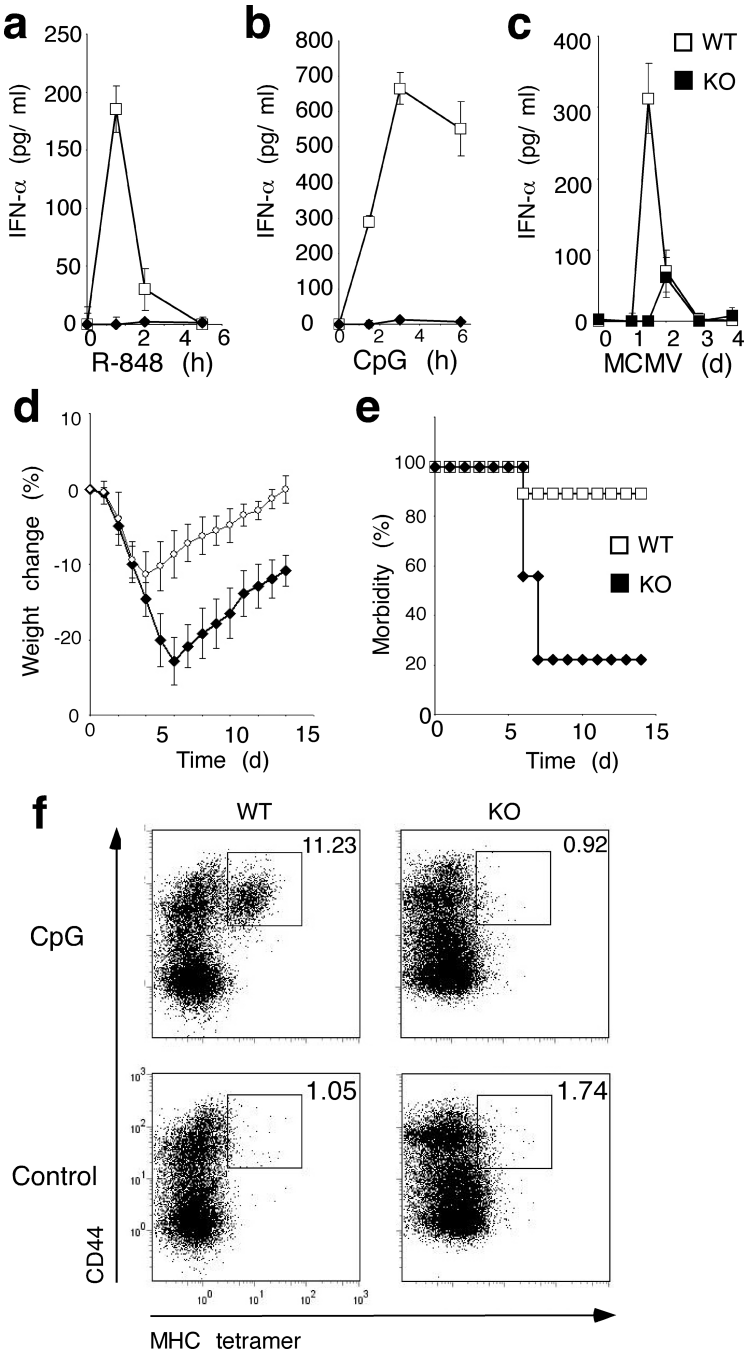

Figure 7. Pin1 is required for TLR-mediated, type I interferon-dependent innate and adaptive immunity *in vivo*

(a-c) Pin1 KO mice completely fail to mount robust IFN-α response upon TLR7 or TLR9 activation. *Pin1* WT and KO mice were injected with 50 nmol of R-848 (i.v.) **(a)**, 5 μg CpG-A complexed to DOTAP (i.v.) **(b)**, or MCMV 5× 10^4 PFU (i.p.) **(c)**, followed by assaying serum IFN-α levels at different time points. (n=3)

(d, e) *Pin1* KO mice are highly vulnerable to viral infection. *Pin1* WT and KO mice were injected with 2.5×10^4 PFU MCMV, followed by monitoring changes in body weights over

time **(d)** or with 10^5 PFU MCMV, followed by monitoring morbidity daily for 14 days (n=6) **(e)**.

(f) *Pin1* KO mice are severely defective in triggering the TLR-mediated, IFN-dependent adaptive immunity. *Pin1* WT and KO mice were immunized with ovalbumin, anti-CD40 and CpG-A complexed to DOTAP and six days later, splenocytes were isolated and subjected to FACS analysis using antibodies against CD8a and CD44 and a MHC tetramer. The data shown were gated on CD8a-positive events and are representative of three independent experiments. The numbers indicate the percentage of tetramer-positive cells relative to the total number of $CD8a^+$ T cells.